Peak effect and its evolution from oxygen deficiency in $YBa_2Cu_3O_{7-\delta}$ single crystals

H. Küpfer, Th. Wolf, C. Lessing, A. A. Zhukov,* X. Lançon, R. Meier-Hirmer, W. Schauer, and H. Wühl
Forschungszentrum Karlsruhe, Institut für Technische Physik, and Universität Karlsruhe, Postfach 3640, D-76021 Karlsruhe, Germany
(Received 3 November 1997; revised manuscript received 9 April 1998)

The current density j in bulk $YBa_2Cu_3O_{7-\delta}$ frequently shows a maximum at fields far above the self-field. The responsible defect structure for this peak effect (PE) are small clusters of oxygen vacancies, impurity atoms, or dopants. The current density caused by these defects is studied during the evolution of the PE. Very pure, twin-free crystals without a $j(B)$ peak after high-pressure oxidation were subsequently oxygen reduced, which increases the pinning strength, i.e., concentration and probable size of the vacancy clusters. The peak that appears first very close below the melting line broadens, increases in height, and shifts to lower fields going from the overdoped into the optimally doped region. Above the peak field B_p the current becomes less sensitive to the growing strength of the defect structure in accordance with a plastic deformation of vortices. In the field region below B_p the very low current density is related to a collective interaction. The transition of this elastic interaction below B_p into a regime of plastic deformation above, initiated by the thermal softening of the shear modulus, results in the rise of the current density. The shift of this transition to lower magnetic fields with increasing oxygen reduction as well as with decreasing temperature is related to the thermal influence on the distribution of pinning energies that result in a temperature-dependent effective concentration of pinning defects. [S0163-1829(98)05229-1]

I. INTRODUCTION

The current density j in bulk $RBa_2Cu_3O_{7-\delta}$ (R = Y,Gd,Tm,Nd) shows frequently a maximum at applied magnetic fields far above the self-field. This peak effect (PE) or fishtail is of great interest from both fundamental and technological aspects of high T_c superconductors. The static and dynamic behavior of vortices are discussed as being responsible for the mechanism causing the PE. The very high current densities at 77 K at this maximum (10^5 A/cm^2, 2 T) are of importance for the application of R 123 bulk material in the medium and higher field region.

There are numerous other $j(B)$ peaks that are related to the twin structure,[1–3] the intrinsic pinning from the CuO planes,[4,5] or to second phase particles.[6,7] In the following we address the PE in R 123 from weakly interacting uncorrelated defects investigated as usual for $B\|c$ and the current flowing within the a,b plane. The development of this PE in pure twin-free single crystals with increasing defect concentration from oxygen deficiency shows a dramatic change of the field dependence of j. For a low concentration, the field B_o, at which the current peak starts to increase with field, is close to the irreversibility field $B_{\rm irr}$. This new feature, which was first preliminary studied in Ref. 8, is accompanied by a field B_p, at which j reaches its maximum, which increases with temperature. This is quite in contrast to the usual observation where B_p increases with decreasing temperature, very similar to the irreversibility field. In crystals with such a common behavior of the PE, the nearly temperature-independent ratio $B_{\rm irr}/B_p$ with sample specific values between 2 and 5 is the basis for the scaling relation of the current. This observation points then to one dominant pinning mechanism, but the corresponding defect structure is still a matter of debate. For this reason, we discuss in Sec. III the defect structure responsible for the PE. The topic becomes even more controversial if the mechanism of the PE is addressed. All models proposed so far for the PE are based on the common $j(B)$ dependence that is only weakly influenced by the defect concentration N. The development of the peak with increasing N—starting from a crystal that does not show any PE—must also be described by the models. Therefore, in Sec. IV the evolution of the peak with increasing oxygen deficiency is investigated in highly pure Y 123 single crystals. In Sec. V the observed nonscaling of the current density is related to a temperature-dependent effective defect concentration that explains the similar evolution of the PE with decreasing temperature and with increasing oxygen deficiency. Finally, this concept is used for the interpretation of the critical point in the phase diagram of the vortex state. The relaxation behavior of these crystals in the B and T region where the PE develops shall be addressed in a subsequent paper.

II. EXPERIMENT

$YBa_2Cu_3O_{7-\delta}$ (Y 123) single crystals were grown from CuO-BaO flux in ZrO_2/Y crucibles by the slow cooling method.[9] Before the growth process, powders of Y_2O_3, $BaCO_3$, and CuO with a purity better than 99.99% were mixed and calcined several times in air between 850 and 880 °C. Crystals were grown in the temperature range 1020–935.7 °C using cooling rates of 0.8–1.0 °C/h. At 935.7 °C the remaining flux has been separated from the crystals by pouring off the flux into a porcelain capsule located inside the furnace. After cooling down to room temperature, the crystals were further annealed in a tubular furnace under flowing oxygen. A second oxidation treatment at 175 bar oxygen for about 300 h followed. The crystals were measured in this highly oxidized state and after various reduction steps. The oxygen content of each state was obtained using the isotherms from Ref. 10 that results in $\delta = 0.007$ for the

TABLE I. Oxygen deficiency δ, transition temperature T_c, and transition width ΔT_c between 0.1 and 0.9 from the normal-state signal and the sizes of the investigated twin-free crystals.

Crystal	δ	$T_c \pm \Delta T_c$ (K)	Size $a\times b\times c$ (mm^3)
#1	0.007	89.9±0.5	0.66×0.66×0.053
	0.03	91.7±0.5	
#2	0.007	89.8±0.6	0.62×0.4×0.046
	0.009	90.5±0.3	
	0.010	90.9±0.4	
	0.011	91.3±0.5	
	0.02	92.0±0.2	
	0.03	92.0±0.6	
	0.04	91.7±0.5	
	0.05	91.9±0.8	
	0.06	92.0±0.9	
	0.07	92.0±0.8	

high-pressure oxidized crystals. Some crystals are nearly twin-free in the as-grown state with a monodomain area of about 80% of their sample sizes. They were investigated by polarized light microscopy and the remaining twinned areas were removed by cutting. Table I gives the δ values, the transition temperature T_c, and the sizes of the two crystals from the same batch that were used for the investigation. As the crystals were too small for a chemical analysis, a semiquantitative ICP-MS analysis was carried through with the remaining flux. Except for Zr and Hf, which were present as the corrosion product $BaZrO_3$, only 200 wt ppm Al could be detected. All other impurity concentrations were found to be below 20 wt ppm.

The magnetic moment m of an induced shielding current was measured with a vibrating sample magnetometer (Oxford Instruments) as a function of the magnetic field B and temperature T in the geometry $B\|c$ where the current flows within the a,b plane. The current was determined from the difference of m between increasing and decreasing magnetic field, $\Delta m \sim j$, measured at a constant electric field $E \sim dB/dt$ of about 0.1 μV/cm at the sample surface. The irreversibility fields correspond to the same E criterion and to a current of 100 A/cm^2. The T_c values were obtained from zero-field-cooled and field-cooled measurements using a field of 5×10^{-4} T.

III. DEFECT STRUCTURE RESPONSIBLE FOR THE PE

In this section a summary is given about the correlation between the PE and the defect structure relevant to pinning. The peak of the current is observed in $RBa_2Cu_3O_{7-\delta}$ single crystals, melt textured samples, ceramics, and thick films, but not in thin films prepared as usual. Irradiation with fast neutrons, protons, heavy ions, electrons, or γ radiation may introduce the PE, and it may enhance the peak present before irradiation or the opposite, or even destroy it. A similar complex behavior, discussed in Sec. IV, is observed for a variation of the oxygen content or doping. The peak is crucially dependent on the defect structure and is not intrinsic to the crystal structure. It may be present in twinned and twin-free

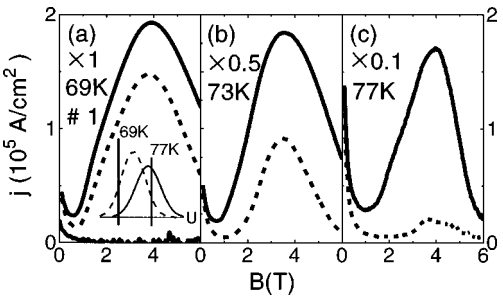

FIG. 1. (a), (b), (c) Current density j vs applied field B for crystal #1 at different temperatures after an oxygen reduction to $\delta = 0.03$. The measurements were made immediately after the reduction (dashed lines) and after the crystal had been stored at room temperature for 5 weeks (solid lines). The current density $<10^4$ A/cm^2 at the bottom of Fig. 1(a) was measured at $\delta = 0.007$. The inset in Fig. 1(a) is explained in the text.

R 123 material.[11,12] In order to make the discussion more clear, we stick to the twin-free single crystals from here on. In the fully oxidized state the current density is low (<500 A/cm^2 at 77 K, 1 T) and decreases monotonously with B without exhibiting a peak. A small oxygen reduction to $\delta=0.04$ produces a very pronounced PE ($>5\times10^4$ A/cm^2 at 77 K, 2 T). From this structure with a large number of pinning centers from oxygen vacancies subsequent oxygenation below 400 °C leads back into the low current state. This completely reversible behavior supports the fact that the PE in these highly pure crystals is caused by oxygen deficiency either by oxygen vacancies or by small oxygen vacancy clusters.[12,13] In less pure crystals the PE results from other kinds of defects, for instance from impurities or dopants. Increasing the number of pinning centers by oxygen reduction in such samples influences j only by means of the reversible properties, but hardly changes its irreversible behavior in the peak region.

Measurements of the magnetic moment vs field B with the angle between the c axis and B as parameter demonstrate that the PE is present in the whole angular regime. Especially for $B\|a,b$, both currents flowing within the a,b plane and along the c axis exhibit the PE.[12] These observations are only in agreement with uncorrelated statistically distributed defects from which the PE results. The interaction strength of these defects must be weak because the PE will be suppressed or vanishes in the presence of strongly interacting defects like correlated twins, uncorrelated second phase precipitates, or large clusters introduced by fast neutron irradiation. The interaction of vortices with the stress field of point defects or small clusters of oxygen vacancies, impurities, or dopants leading to uncorrelated weak pinning is in accordance with the experimental findings.

In the case where the PE develops from oxygen reduction as in pure crystals, oxygen vacancies can be excluded as the responsible defect structure from the following observation. The twin-free crystals in the highly oxidized state show, above 70 K, a monotonously decreasing current with field. Then the crystals were deoxidized and afterwards rapidly cooled down to room temperature. The dashed lines in Figs. 1(a)–1(c) that represent the current density measured immediately after the reduction show at 77 K a very weak current maximum [Fig. 1(c)]. Then the crystal was stored at room

temperature for about 5 weeks, which does not change its oxygen content but allows a short scale diffusion of oxygen vacancies. This results in small clusters of oxygen vacancies presumably as a precursor of an oxygen ordering.[14] The current resulting from these defects shows a well pronounced PE at 77 K [solid line in Fig. 1(c)] demonstrating that point defects—at least oxygen vacancies—do not cause the peak, in agreement with Erb *et al.*[13] The difference between the currents before and after aging decreases at lower temperatures [Figs. 1(a) and 1(b)]. At 69 K, for instance, the peak was present also before aging but not before oxygen reduction [solid line at the bottom of Fig. 1(a)].

This observation is explained by assuming a defect size distribution ranging from point defects to larger clusters resulting in a distribution of the pinning energy U. The pinning potential of point defects is smeared out above 50 K by the thermal oscillation of vortices. The depinning line, which is determined by the energy of about kT, is now situated within the distribution of pinning energies (DPE's). The pinning energy of point defects is on the lower and the one of the clusters is on the higher energy part of the DPE. Therefore, the effective density of the interacting defects (N_{eff}) with a pinning energy larger than kT becomes smaller with increasing temperature. At 69 K, N_{eff} is sufficiently large to cause the PE also immediately after oxygen reduction [dashed line in Fig. 1(a)]. Increasing temperature decreases N_{eff} of these defects to about zero at 77 K where only a small PE occurs [dashed line in Fig. 1(c)]. However, the same defects already cause at 69 K an increase from about zero current to a pronounced peak. This means that at 69 K the depinning line lies in the low-energy part and at 77 K in the high-energy part of the DPE. After room-temperature aging, the DPE shifts to higher pinning energies and the depinning line for 77 K is now fully within the distribution. The inset in Fig. 1(a) demonstrates, for 69 and 77 K, qualitatively this explanation. For simplicity, the temperature dependence of the DPE is neglected. The number of effective pinning centers increased at 77 K, much more than at 69 K, which explains the larger rise of the current at 77 K. This explanation is further in accordance with the observation that crystals that do not have a PE in the higher temperature region show this feature with decreasing temperatures due to pointlike defects or clusters different from oxygen defects. Such a temperature-dependent effective concentration of pinning centers prevents a scaling behavior of the current which, indeed, is not observed in the temperature region shown in Figs. 1(a)–1(c) as discussed in Sec. V.

Another observation additionally rejects point defects being the origin of the PE. One crystal was exposed to γ radiation from a ^{60}Co source up to a dose of 10^7 rad. Besides oxygen vacancies and interstitials, other point defects are introduced that are not mobile at room temperature, i.e., they do not agglomerate to small clusters. The current is increased by about 10% due to these added pinning centers, but only at lower temperatures. In the higher temperature region, the radiation induced point defects do not affect j and they especially do not change the PE. This finding is in full agreement with the result above, that in the higher temperature region point defects are not able to introduce the PE.

IV. EVOLUTION FROM OXYGEN DEFICIENCY

Several mechanisms were proposed for the origin of the PE in high- and also in low-T_c superconductors. The majority of models are based on weak elementary pinning forces resulting in low currents at fields below which j starts to increase. But all these models differ in their explanation given for the anomalous rise of the current up to B_p, and they also partly differ in their explanations for the decrease of j above B_p. Weak elementary pinning forces cause an elastic collective interaction with the vortex lattice. This interaction is characterized by the size of a correlation volume $V_c = R_c^2 L_c$ (Refs. 15 and 16) within which the order of the vortex lattice is still established: R_c is the transverse and L_c the longitudinal size. The transverse size should transform with increasing field from the single vortex collective regime ($R_c < a$) via the small bundle ($\lambda > R_c > a$) into the large bundle regime ($\lambda < R_c$); $a \sim B^{-1/2}$ is the vortex lattice spacing. The field dependence of the current is determined by the field dependence of V_c to be $j \sim V_c^{-1/2}$.

In the static collective pinning theory,[15] thermally activated relaxation, and the single vortex collective regime, as well as the small bundle regime, are not considered. The rise of the current is related to the decrease of V_c from the large bundle to the single vortex regime. The transition starts at a field B_0 at which R_c becomes equal to the effective penetration depth $\lambda_{\mathrm{eff}} = \lambda/(1-B/B_{c2})^{1/2}$ and is completed at B_p. The origin for this change from a local ($R_c > \lambda_{\mathrm{eff}}$) to a nonlocal interaction ($R_c < \lambda_{\mathrm{eff}}$) is the dispersion of the tilt modulus C_{44}.

In the dynamic model[17] for the PE based on the collective creep theory,[16] the increase of j is related to the transition from the single vortex collective state with a high relaxation rate into the small bundle region with a lower relaxation. In this case the unrelaxed current is expected to decrease monotonously with B and the PE is caused by the larger thermally activated decay of j in the low-field single vortex collective regime where the interaction between vortices is negligible. This dynamic interpretation is opposite to all the static models in which both the relaxed and the unrelaxed currents are expected to show a PE. In the static case, relaxation influences only the B and T dependences of the current, but the PE is caused by a different mechanism.

In another frequently used explanation, the increase of j is directly related to an increase of the strength of the elementary pinning forces.[18,19] This is based on the assumption that a distribution of oxygen deficient regions acts as pinning sites that are superconducting below B_0 and reach their normal or reversible state for B approaching B_p. The decrease of j above B_p is related to granularity from overlapping of the normal or reversible regions.

Two earlier explanations leading to an increase of the current with B are a softening of the elastic moduli or a synchronization of the vortex lattice.[20,21] These mechanisms are not necessarily based on an elastic interaction of weak elementary pinning forces.

The defect concentration N is in none of these models a sensitive parameter with respect to the field dependence of the current. In the static collective pinning theory the fields B_0 and B_p decrease with increasing N because R_c shrinks with a larger defect concentration.[15] Further, the parameter N

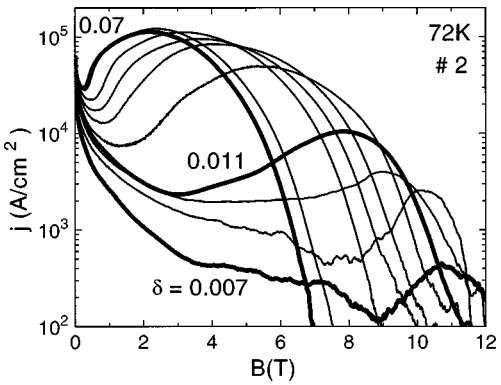

FIG. 2. Current density j vs applied field B at 72 K in crystal #2 measured at different oxygen deficiencies δ from 0.007 to 0.07 as given in Table I.

is not at all discussed because comparisons between theories and measurements are made on samples in which the concentration is high and variations of N are of minor influence, i.e., the PE has its well-known field dependence. In very pure crystals, however, a variation of the defect concentration allows a more detailed check of the proposed explanations for the PE. In the following, the evolution of the peak with increasing N from oxygen reduction is discussed in naturally twin-free, pure Y 123 single crystals. After high-pressure oxygen loading, these samples show in the higher temperature region a very small and monotonously decreasing current with field. This about reversible behavior is in agreement with resistive measurements in the transition regime from the vortex liquid into the solid state demonstrating a vortex melting behavior.[22] From this overdoped regime ($\delta = 0.007$) the crystals were subsequently deoxidized down to $\delta = 0.07$, which is about the optimally doped region. During this reduction, T_c approaches its maximum value, the transition from the solid into the liquid vortex phase decreases to lower values, the B, T critical point up to which a first order transition is present decreases to zero magnetic field at T_c, and the concentration of oxygen vacancy clusters becomes higher by about one order in magnitude. For instance for $\delta = 0.017$ the concentration of the introduced oxygen vacancies is 10^{20} cm^{-3}. Assuming a minimum cluster volume of ten unit cells results in an upper limit for the cluster concentration of about 10^{19} cm^{-3}. Further uncertainties come from the size distribution, a possible oxygen ordering, and from different point or pointlike defects already present in the fully oxidized state. These defects may act as sinks for the oxygen vacancies and therefore grow in size with δ. This shifts their pinning energies to the higher temperature region. Furthermore, oxygen vacancy clusters may also become larger in size with further oxygen reduction, changing the DPE and preventing a linear dependence between δ and the defect concentration. At present, the knowledge about this defect structure is very poor. Therefore, in the following we discuss, for reasons of simplicity, only the rise of the concentration of oxygen defect clusters with increasing δ, knowing that, in principle, all the variations mentioned above are involved.

Figure 2 shows the development of the PE with δ from 0.007 to 0.07 at $T = 72$ K for crystal 2 as an example. At $\delta = 0.007$, 72 K is the highest temperature where the peak is

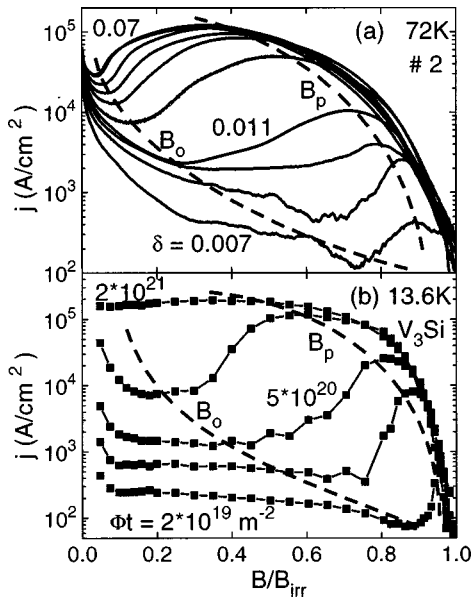

FIG. 3. (a), (b) Current density j vs applied field divided by the irreversibility field, $B/B_{\rm irr}$, for crystal #2 (3a) at 72 K. The dashed lines are guides to the eye demonstrating the shift of the fields B_p and B_0 to lower values with increasing δ. Fig. 3(b) shows the same development of the peak effect in V_3Si at 13.6 K from Ref. 25. Here the fast neutron fluence that is proportional to the defect cascades was increased from 2×10^{19} m^{-2} to 2×10^{21} m^{-2}.

above the noise level. It is situated close below the melting line that is about 12 T. With increasing δ, the peak broadens, increases in height, and shifts to lower fields. It approaches its common field dependence for δ larger than about 0.03. In the field region above the peak field B_p, the current becomes less sensitive to the increasing defect concentration. This phenomenon becomes more pronounced if one accounts for the decreasing melting fields with increasing δ. This is approximately done by reducing the field with the corresponding irreversibility fields [Fig. 3(a)]. Such a saturation behavior is expected if, for instance, the pinning force becomes larger than the shear force between vortices that then determines the current. The saturation is experimental evidence for a plastic deformation leading to a highly disordered or an amorphous flux state that can be characterized by $R_c \approx a$ above B_p. For δ above 0.03, the field dependence above B_p starts to change, i.e., the saturation does not result in one single curve in the higher field region of Fig. 3(a). We relate this deviation to a lower increase of the concentration due to the growing size of the defects with δ.

The evolution of the peak starting close below the melting point is in agreement with the softening of the effective shear modulus that approaches zero at the melting field B_m. This explanation, interpreting the peak to be a precursor of melting, was drawn from resistive measurements made in quite different low- and high-T_c superconductors[1,23,24] where a very sharp increase of the current just below B_m is observed. The measurements shown in Fig. 2 are the first observations that the same phenomenon occurs for the PE in Y 123. The low currents in the field region up to B_o where j starts to increase are related to an elastic vortex interaction with a large V_c, in satisfying agreement with results from relaxation measurements. The decreasing effective shear modulus

C_{66}^{eff} initiates the transition from the elastic to the plastic deformation. It allows larger displacements of the flux lines, the correlation volume shrinks and the pinning force that is proportional to j starts to increase. At about B_p the transverse size R_c is reduced to its minimum value. Above this field, in the single vortex noncollective interaction region, j is expected to be determined either by the pinning force or by the shear force between vortices. If a saturation is observed the shear force must be overcome by the pinning force above B_p. The shear force is expected to have a field dependence determined by the effective shear modulus. It is zero at B_{c1} and B_m, and has a maximum in between. From B_o to B_p, a transformation from the elastic collective interaction below B_o to the plastic deformation of the flux lattice above B_p takes place. This is equivalent to a change from a flux lattice with low disorder to an amorphous or glassy state. In nearly defect-free crystals this transformation should happen close to B_m in agreement with the observations from resistive measurements. With increasing N, static disorder is added to the thermal disorder of the flux lattice. As a consequence the shear force decreases and simultaneously the pinning force increases. For both reasons, the fields B_o and B_p are shifted towards lower values and a broadening of the peak as well as an increase in height is expected. This evolution with increasing N is almost finished if the concentration exceeds a certain value above which the shear force determines the current in the whole field regime except at low fields where stronger interacting defects are dominating. In this final state, above $\delta = 0.03$, the PE shows its well-known field dependence.

The evolution of the PE in Y 123 is further in some qualitative agreement with the development of the peak in low-T_c superconductors. For instance, in V_3Si, with defects from fast neutron irradiation, the $B_o(N)$ and $B_p(N)$ dependences are similar [Fig. 3(b)]. In the field region below B_p, there is even a quantitative agreement with the static collective pinning model.[25] At fields above B_p, a pronounced saturation behavior is also present. In the field region between B_o and B_p, history effects of the current density support here, in addition, the transition from a crystalline to an amorphous state of the flux lattice. The static collective model is based on a melting field very close to B_{c2}. This is quite different in Y 123 with $B_m \ll B_{c2}$ and a decrease of C_{44} with B probably far above B_m. But from a more general point of view the softening of C_{44} towards B_{c2} may be replaced by the thermally activated decrease of the effective shear modulus towards B_m or B_{irr}. With a corresponding condition for B_o and replacing B_{c2} by B_{irr}, the behavior of $j(B,N)$ in Y 123 can be transferred to the peak in low-T_c superconductors, i.e., the evolution of the PE with defect concentration in V_3Si is equivalent to the PE from oxygen vacancy defects in Y 123. Different modifications of the static and dynamic collective pinning model were discussed in Refs. 26 and 27 for explaining the PE in its fully developed state.

The occurrence of the peak close to B_m rejects the relaxation model[17] based on the collective creep theory as the origin of the PE because it would require a single collective vortex regime extended close to the melting line. Further, the region of plastic deformation above the peak field, verified by the saturation, is inconsistent with any elastic interaction regime that should follow the small bundle regime above B_p.

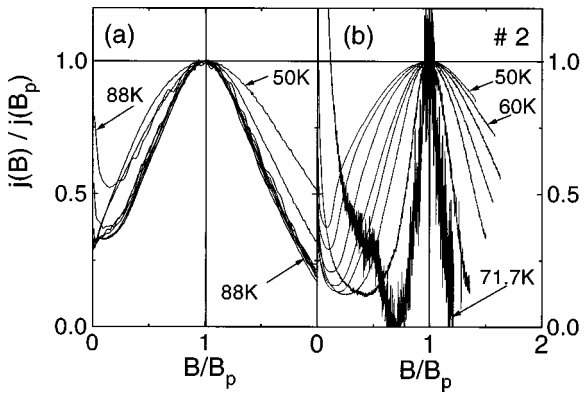

FIG. 4. (a), (b) Normalized current density j vs normalized applied magnetic field at different temperatures. The crystal in Fig. 4(a) shows a scaling behavior in contrast to crystal #2 [Fig. 4(b)].

The change of the pinning mechanism between B_o and B_p is also indicated by a change of the $E(j)$ characteristics in this field region.[28] Below B_o $\ln E$ vs $\ln j$ shows a negative curvature which corresponds to a positive exponent μ in qualitative agreement with an elastic interaction from collective creep or with the vortex glass state. But, in the field region above B_p, $E(j)$ characteristics show a power-law dependence or even a positive curvature that corresponds to negative μ values in agreement with a single vortex noncollective interaction. A similar observation of a transition from an elastic to a plastic deformation was recently made by Abulafia *et al.*[29] using local relaxation measurements.

V. SCALING BEHAVIOR AND PHASE DIAGRAM

The temperature scaling of the current $j(B,T)/j(B_p,T) = f(B/B_p)$ is a well-known property in twinned and twin-free crystals. An example is shown in Fig. 4(a). The temperature-independent scaling function f hardly depends on the kind of defects causing the PE. Deviations from the scaling behavior may result from different origins. In the higher temperature region the pinning interaction of twins and other large scale defects suffer less from thermal oscillations of the vortices than pointlike defects or the oxygen vacancy clusters. Then these two- or three-dimensional defects become dominant and cause an upward turn of the scaling function at low fields [Figs. 4(a) and 4(b) at 88 and 71.7 K, respectively]. Violation of the scaling at lower temperature can be caused by the channeling of vortices along twin walls or alternatively due to an enhanced effective tilt modulus of the vortex lattice.[30–32] This results in a depression of the current around B_p, leading in some crystals to a $j(B)$ plateau. Also, twin-free crystals always show a broadening of the peak at lower temperatures because the effective defect concentration increases with decreasing temperature. All these interferences, as well as the transition width at T_c, determine a temperature window from about 60 to 80 K where a satisfying scaling behavior of the current with a PE is usually observed. However, in the twin-free crystals where the PE starts to evolve from oxygen reduction, no scaling is observed, in particular not in this temperature window as demonstrated in Fig. 4(b). With increasing temperature the

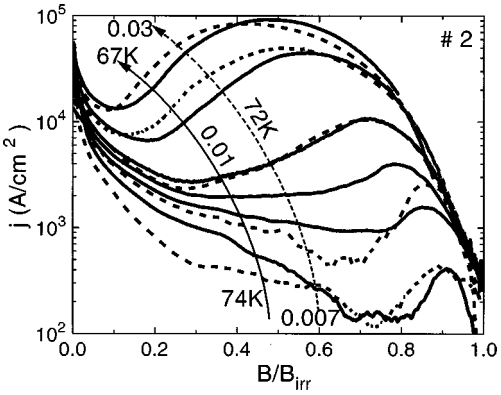

FIG. 5. Current density j vs applied field divided by the irreversibility field, B/B_{irr}, for a constant δ of 0.01 at $T=74$, 73, 72, 68, and 67 K (solid lines). The evolution of the peak effect is very similar for a constant T of 72 K at $\delta=0.007$, 0.009, 0.01, 0.011, 0.02, and 0.03 (dashed lines).

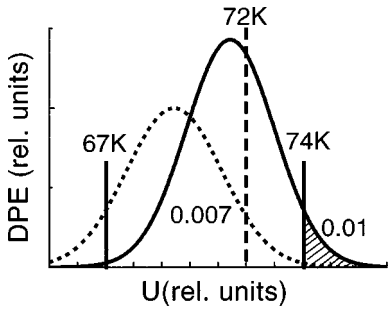

FIG. 6. Schematic drawing of the distribution of the pinning energy DPE vs pinning energy U for $\delta=0.01$ (solid line) and 0.007 (dashed line). The concentration of effective pinning sites with $U>kT$ is given by the shaded area for 0.01 at 74 K as an example. This concentration results in the same peak effect as for $\delta=0.007$ at 72 K (dashed line).

width of the peak shrinks and its position shifts towards the irreversibility line. The temperature dependence of B_p and B_o that is above 60 K opposite to $B_{\mathrm{irr}}(T)$ prevents the scaling behavior where the PE develops. Usually a nonscaling of the current may point to a comparable strength of two or more defect structures with different temperature dependences. If, however, one defect structure dominates, violation of scaling may indicate a change of the pinning mechanism due to a crossover between the characteristic length scales of the superconductor and the defect structure. Both possibilities do not fit to the nonscaling behavior in Fig. 4(b). Further, this unexpected feature is not intrinsic to the development of the PE because low-T_c superconductors show a very good scaling in this region where the peak evolves.[25] The present nonscaling behavior of the current with decreasing T at a constant δ reminds one, however, of the evolution of the peak with increasing δ or N at a constant temperature. This correspondence is demonstrated in Fig. 5 where $j(B/B_{\mathrm{irr}})$ is shown at $\delta=0.01$ with T as parameter (solid lines) and for comparison at $T=72$ K with δ as parameter (dashed lines). The evolution of the PE at $\delta=0.01$ occurs from 74 to 67 K equivalent to the oxygen reduction from 0.007 to 0.03 at 72 K. For each δ below 0.04 there exists a temperature region in which with decreasing T the PE develops equivalently as with increasing δ. A lower δ value requires for this correspondence a higher temperature region and vice versa. This similarity points to an effective defect concentration N_{eff} that increases with decreasing temperature as already briefly explained in Sec. III. The pinning energy U from the oxygen defects is assumed to have a DPE. Thermal oscillations of the vortices reduce the maximum gradient of the effective pinning potentials and broaden the distribution. Relaxation measurements result in S values between 0.3 and 0.5 in the B and T areas under discussion. Therefore, kT can be expected to be within the distribution where pinning sites below kT do not contribute to the current. Only the number of pinning sites N_{eff} with $U>$kT is essential for the interaction with the vortex lattice. The effective concentration rises with larger δ values at constant T as usual, but it increases also with decreasing temperatures at constant δ, i.e., a constant absolute density of oxygen defects. This behavior is qualitatively illustrated in Fig. 6. The same tiny PE is obtained for 0.007, 72 K, and for 0.01, 74 K (Fig. 5) and a pronounced one for 0.01, 67 K. Consequently, the DPE in Fig. 6 for 0.01 (solid line) results above 74 K in the same low N_{eff} (shaded area) as the DPE for 0.007 above 72 K (dashed line). However, at 67 K kT is at the low-energy side of the DPE for 0.01, N_{eff} is large and the PE is about fully developed. This equivalent influence of δ and T on N_{eff} is further quantified in Fig. 7 where the current at B_p is shown at $\delta=0.01$ vs T and at $T=72$ K vs $1-\delta$. Both the δ and the T scales are linear, which results in $N_{\mathrm{eff}}\ (1-\delta)\sim N_{\mathrm{eff}}(T)$, valid in the temperature range where kT is within the DPE. Such a possibility of a temperature-dependent N_{eff} prevents a scaling behavior of the current because the dependence of the current on the concentration of the active pinning sites is different in different magnetic-field regimes. For instance, B_p and B_o are shifted to lower values with increasing N_{eff}. Further, in this field region between B_o and B_p the influence of the concentration on j is much stronger than below B_o and above B_p. This nonscaling behavior of the current is restricted to the higher temperature range where B_o and B_p exhibit a temperature dependence opposite to B_{irr} or B_m. In the lower temperature region, below the minimum of $B_p(T)$, the scaling of j becomes much better. Here kT is expected to be below the DPE, i.e., all pinning sites contribute to the current and N_{eff} is no longer temperature dependent. For defect structures where kT is below the DPE up to B_{irr}, the PE

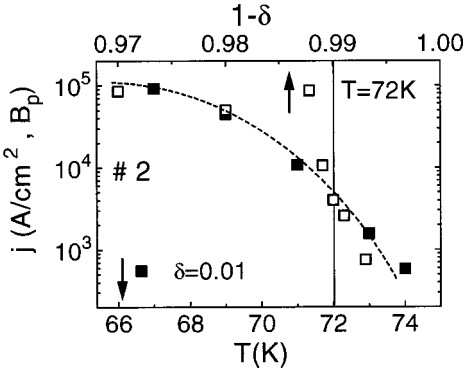

FIG. 7. Current density j at the peak field B_p for a constant δ of 0.01 vs temperature T (filled squares) and for a constant T of 72 K vs oxygen deficiency 1-δ (open squares). The dashed line is a guide to the eye demonstrating the good agreement between both.

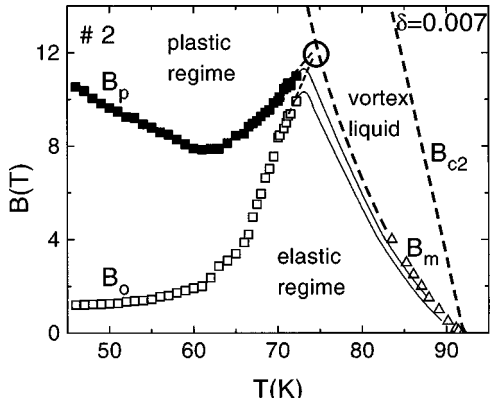

FIG. 8. Temperature dependence of fields at which the current density j passes its maximum (B_p), and at which j starts to increase (B_0). $B_m(T)$ is the melting line and $B_{c2}(T)$ the upper critical field. The solid lines are explained in the text. The measurements are made in crystal #2 with an oxygen deficiency of $\delta=0.007$.

is fully developed and scaling may be observed in the whole temperature range. This explanation for the nonscaling behavior is equivalent to assume a depinning line with a different temperature dependence than the pinning energies or their distribution. If the DPE is above the depinning line, scaling is observed whereas if it is within the distribution scaling fails.

The evolution of the PE with decreasing temperature at a constant δ (solid lines in Fig. 5) rejects the frequently proposed model of the origin of the peak based on the elementary pinning force. In this explanation the peak field corresponds to the field where the superconducting region become normal conducting or reversible. But B_p decreases with decreasing temperature quite opposite to any phase boundary between superconducting and normal conducting or reversible state.

To summarize the discussion of Sec. V, a plot of the B,T plane is shown in Fig. 8. The vortex liquid phase extends from B_{c2} to B_m (dashed lines). The melting line was measured up to 4 T. The elastic interaction regime is settled below B_o and the plastic deformation above B_p. In between, the current increases with B and the vortex lattice transforms from a large bundle regime to a single vortex state above the peak field. This change of disorder is accompanied by a change of the $E(j)$ characteristics. The nonscaling behavior of the current is present in the temperature region above 60 K where B_p and B_o increase with T. Below the minimum of the peak field $(B_p)_{\min}$, the scaling improves with decreasing temperature. In this region we expect an effective defect concentration approaching a constant value independent of T, whereas above 60 K $N_{\rm eff}$ decreases with increasing temperature. This temperature dependence of $N_{\rm eff}$ is also supported by the collective pinning model. The field B_o is predicted by the equation $R_c\ (B_o)=\lambda/(1-B_o/B_{c2})^{1/2}$ where R_c is proportional to the inverse defect concentration.[15] If a scaling behavior holds, $b_o=B_o/B_{c2}$ is temperature independent and a plot of $[1-b_o(T)]^{1/2}$ should be independent of T and proportional to the effective defect concentration. Replacing B_{c2} by the extrapolated $B_{\rm irr}$ values, $[1-b_o(T)]^{1/2}\sim N_{\rm eff}$ increases from 70 to 60 K by about one order of magnitude. Below 60 K this rise becomes much smaller. The minimum of the peak field coincides with the temperature below which $N_{\rm eff}$ becomes about constant and a scaling is observed. This correlation is not obvious because B_p does not enter the above relation.

The (B,T) point where the depinning line is entirely above the DPE and $N_{\rm eff}$ becomes zero, is close to B_m for an oxygen deficiency of $\delta=0.007$ (Fig. 8). The temperature dependences of B_o and B_p in this region where the magnetic moment is no longer accessible for experimental restrictions depend on whether (B,T) for vanishing $N_{\rm eff}$ is in the vortex solid or in the liquid regime. In the first case the temperature dependences are given by extrapolations of $B_o(T)$ and $B_p(T)$ (dashed lines) that then meet each other in the vicinity of B_m (circle in Fig. 8). The temperature dependences in the other case, where this point of zero effective pinning sites is in the vortex liquid regime, are indicated by the two thin solid lines in Fig. 8. Immediately below the melting line each defect structure causes a plastic interaction with the vortices that transforms to an elastic interaction when with decreasing B or T the effective shear modulus of the vortices rises. This second possibility is supported by resistive measurements[22] where a small dip in the resistivity below B_m points to a PE also for $T>83$ K. This observation is similar to results from resistive measurements in low-T_c superconductors and in very clean Y 123 crystals where a small number of twin planes causes a PE as a precursor of melting.[1] We are not able to exclude the presence of remaining twins in our crystals. Therefore, the PE above 75 K may alternatively result from such a defect structure different from oxygen vacancy clusters. Then, around 75 K both peaks caused by different defects merge with each other. In both cases the same sequence is present below the melting point: plastic deformation, the peak, and then the elastic regime. In this discussion, related to the region close to B_m, pronounced relaxation is also expected to influence strongly the B and T dependences of the PE.

Recently, the phase diagram of the vortex matter in Y 123 was discussed by Deligiannis *et al.*[33] The B,T region (circle in Fig. 8), where the extrapolated B_p meets B_m, was related to a multicritical point as observed in Bi 2212.[34] In the present interpretation this point is governed by the interplay between the DPE and kT. It separates weak disorder in the vortex structure below from a strong one above due to the change of the effective defect concentration in the vicinity of this point. This is in accordance with a first-order transition from the vortex liquid into the solid state below and a second one above the critical point. But in this picture the critical point may vanish completely if the defect concentration decreases further. In this case $(B_p)_{\min}$ is expected to shift to higher fields with lower temperatures. The (B,T) point with $N_{\rm eff}=0$ may then be situated in the solid phase and not at the border. The PE may therefore vanish before reaching B_m and a first-order transition is expected also for higher fields or lower temperatures.

This interpretation is consistent with the experimental observation of $B_p(T)$ if the defect structure from oxygen vacancies is increased going from the overdoped into the optimally doped region. The development of $B_p(T)$ from this oxygen reduction is shown in Fig. 9. With increasing δ from 0.007 the temperature at which B_p passes its minimum is

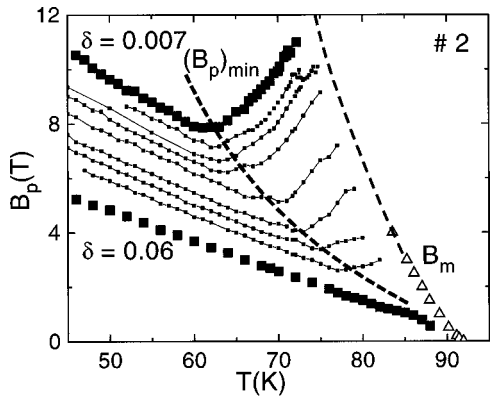

FIG. 9. Field B_p at which the current density j passes its maximum vs temperature T for crystal #2 at different δ values from 0.007 to 0.06 as given in Table I.

shifted towards the melting line. At about $\delta = 0.06 (B_p)_{\min}$ approaches B_m and the critical point vanishes. At this reduction step, where the temperature region between $(B_p)_{\min}$ and B_m becomes about zero, the scaling behavior starts to improve considerably. This is related, as discussed above, to an increase of N_{eff} with δ. In the final state the DPE is above kT and the effective concentration becomes constant. The PE is then fully developed, scaling is observed close up to T_c, and the peak field and B_o increase monotonously with decreasing temperature. As a consequence of the larger disorder in the vortex lattice the first-order melting transition has changed into a second-order transition at this reduction step. The irreversibility line is considerably lower than the melting line observed at lower δ values. As discussed above, $(B_p)_{\min}$ is related to the condition where kT is below the DPE. Therefore, the increase of $(B_p)_{\min}$ towards B_p is caused by a shift of the DPE to higher energies from the growth of the oxygen clusters with δ.

VI. SUMMARY

The maximum of the current density j vs magnetic field B (peak effect or fishtail) is investigated in $YBa_2Cu_3O_{7-\delta}$ single crystals with different values of the oxygen deficiency δ. Oxygen reduction results in an isotropic uncorrelated defect structure interacting with the vortices. In very clean crystals the PE vanishes after high-pressure oxidation. With increasing oxygen reduction, however, the PE reappears and evolves to its usual $j(B)$ dependence. Oxygen vacancies can be excluded as being the responsible pinning sites at high temperatures. The current, measured immediately after oxygen reduction and fast cooling to room temperature, increased considerably in the field region of the peak after the crystal had been stored at room temperature for several weeks. This room-temperature aging, which does not change δ but allows the diffusion of oxygen vacancies, results in the formation of small oxygen vacancy clusters. In less pure crystals other weakly interacting defects from doping or impurities are the responsible defect structure for the PE. In these samples oxygen reduction is of minor or even negligible influence on the $j(B)$ dependence.

The pinning interaction between these defects and the vortices, resulting in the anomalous rise of the current with increasing B, cannot be studied in twinned crystals. The influence of the strongly interacting, correlated twin structure on the B and T dependence of the current and its relaxation exerted from the weakly interacting defects, is much too strong. For this reason, naturally twin-free crystals were used that show a first-order melting transition from the solid into the liquid state of the vortices. These crystals show after high-pressure oxidation a very tiny PE close to the irreversibility or melting line. With subsequent oxygen reduction the peak broadens and increases in height. The peak field B_p at which j has its maximum, and the field B_o at which j passes its minimum before it increases towards B_p, both shift to lower values with δ, i.e., with increasing concentration of oxygen vacancy clusters. Below B_o, relaxation rates and voltage current characteristics are in agreement with a collective pinning interaction. The observation that B_o is close to B_{irr} excludes a single vortex collective regime but favors a large bundle regime below B_o with a transverse size R_c of the correlation volume V_c larger than the London penetration depth λ. This is in qualitative agreement with the very low and monotonously decreasing current with B up to B_o, i.e., a large and increasing $V_c(B)$ with a maximum R_c at B_o.

Above B_p the current becomes nearly independent of the rising strength of the defect structure. Such a saturation behavior is a strong indication for a plastic deformation of the vortices that results in a large disorder. This plastic deformation in the region between B_p and B_{irr} is expected also from the effective shear modulus of the vortex lattice that vanishes at the transition into the liquid state. The two regimes, elastic interaction below B_o with $R_c \gg \lambda$ and plastic deformation above B_p, result naturally in a maximum current in the transition region where R_c approaches its minimum value. This mechanism is discussed already as a precursor of melting in low- and high-T_c superconductors showing a very tiny peak in resistive measurements immediately below the melting line. The result of our investigation demonstrates that the same development is responsible for the fishtail or peak effect. Then, with increasing strength of the defect structure from oxygen reduction, the disorder in the vortex lattice increases and its amorphous regime broadens towards lower fields.

The development of the PE in twinned crystals is quite different due to the constraints of R_c by the twin spacing in the elastic interaction regime. If this influence is strong B_o is absent and appears only outside the trapping angle of the twins.

The evolution of the peak with increasing pinning strength from oxygen reduction at constant T is equivalent to its evolution with decreasing temperature at constant δ. This behavior is related to an increasing effective defect concentration with decreasing temperature caused by a distribution of the pinning energies. The thermal energy kT that lies within this distribution prevents the pinning sites with $U < \text{kT}$ from contributing to the current. A scaling behavior of the current is only observed in the temperature region where kT is below this distribution and, therefore, the effective concentration of oxygen vacancy clusters becomes temperature independent.

The so-called critical point where the melting line and the peak field meet each other is, in this interpretation, caused by

the effective defect concentration that decreases with temperature. Therefore the regime of elastic vortex interaction extends to higher fields and approaches the melting line at larger B_m. Increasing strength of the defect structure then results in a lower critical point that vanishes if the region of elastic vortex interaction decreases monotonously with temperature.

ACKNOWLEDGMENTS

This work was partly supported by the cooperation program between the Deutsche Forschungsgemeinschaft (Grant No. 436 RUS 113/417/0) and the Russian Fund for Basic Research (Grant No. 96-02-00235G). We would like to thank Mrs. A. Will and Mrs. B. Runtsch for performing VSM measurements and for technical assistance.

*Also at Physics Department, Moscow State University, Moscow 117234, Russia.

[1] W. K. Kwok *et al.*, Phys. Rev. Lett. **73**, 2614 (1994).
[2] L. M. Fisher *et al.*, in *Proceedings of the EUCAS 1995*, edited by D. Dew-Hughes, IOP Conf. Proc. No. 148 (Institute of Physics, and Physical Society, Bristol, 1995), p. 319; A. A. Zhukov *et al.*, Phys. Rev. B **56**, 3481 (1997).
[3] Th. Wolf *et al.*, Phys. Rev. B **56**, 6308 (1997).
[4] M. Oussena *et al.*, Phys. Rev. Lett. **72**, 3606 (1994).
[5] H. Küpfer *et al.*, in *Proceedings of the 8th International Workshop on Critical Currents in Superconductors*, edited by T. Matsushita and K. Yamafuji (World Scientific, Singapore, 1996), p. 373.
[6] M. Murakami *et al.*, in *Proceedings of the 8th International Workshop on Critical Currents in Superconductors* (Ref. 5), p. 57.
[7] M. R. Koblischka *et al.*, Phys. Rev. B **54**, R6893 (1996).
[8] H. Küpfer *et al.*, in *Proceedings of the 8th International Workshop on Critical Currents in Superconductors* (Ref. 5), p. 3499.
[9] Th. Wolf *et al.*, J. Cryst. Growth **96**, 1010 (1989).
[10] D. J. L. Hong and D. M. Smith, J. Am. Ceram. Soc. **74**, 1751 (1991).
[11] A. A. Zhukov *et al.*, Phys. Rev. B **51**, 12 704 (1995).
[12] H. Küpfer *et al.*, Phys. Rev. B **54**, 644 (1996).
[13] A. Erb *et al.*, J. Low Temp. Phys. **105**, 1033 (1996).
[14] M. Daeumling *et al.* (unpublished).
[15] A. I. Larkin and Yu. N. Ovchinnikov, J. Low Temp. Phys. **34**, 409 (1979).
[16] G. Blatter *et al.*, Rev. Mod. Phys. **66**, 1125 (1994).
[17] L. Krusin-Elbaum *et al.*, Phys. Rev. Lett. **69**, 2280 (1992).
[18] M. Daeumling *et al.*, Nature (London) **346**, 332 (1990).
[19] L. Klein *et al.*, Phys. Rev. B **49**, 4403 (1994).
[20] A. B. Pippard, Philos. Mag. **19**, 217 (1969).
[21] J. Kramer, J. Appl. Phys. **44**, 1360 (1973).
[22] C. Lessing, Diploma thesis, University Karlsruhe, 1996.
[23] S. Bhattacharya and M. J. Higgins, Phys. Rev. Lett. **70**, 2617 (1993).
[24] N. R. Dilley *et al.*, Phys. Rev. B **56**, 2379 (1997).
[25] R. Meier-Hirmer *et al.*, Phys. Rev. B **31**, 183 (1985).
[26] R. Hiergeist and R. Hergt, Phys. Rev. B **55**, 3258 (1997).
[27] V. M. Pan *et al.*, Physica C **279**, 18 (1997).
[28] H. Küpfer *et al.*, Phys. Rev. B **50**, 7016 (1994).
[29] Y. Abulafia *et al.*, Phys. Rev. Lett. **77**, 1596 (1996).
[30] M. Oussena *et al.*, Phys. Rev. B **51**, 1389 (1995).
[31] A. A. Zhukov *et al.*, Phys. Rev. B **52**, R9871 (1995).
[32] V. F. Solovjov *et al.*, Phys. Rev. B **50**, 13 724 (1994).
[33] K. Deligiannis *et al.*, Phys. Rev. Lett. **79**, 2121 (1997).
[34] B. Khaykovich *et al.*, Phys. Rev. Lett. **76**, 2555 (1996).